

A standalone perfusion platform for drug testing and target validation in micro-vessel networks

Boyang Zhang,^{1,2} Carlotta Peticone,¹ Shashi K. Murthy,^{3,4}
and Milica Radisic^{1,2,a)}

¹Department of Chemical Engineering and Applied Chemistry, University of Toronto,
Toronto, Ontario M5S 3E5, Canada

²Institute of Biomaterials and Biomedical Engineering, University of Toronto, Toronto,
Ontario M5S 3E2, Canada

³Department of Chemical Engineering, Northeastern University, Boston, Massachusetts
02115, USA

⁴Barnett Institute of Chemical & Biological Analysis, Northeastern University, Boston,
Massachusetts 02115, USA

(Received 3 June 2013; accepted 31 July 2013; published online 26 August 2013)

Studying the effects of pharmacological agents on human endothelium includes the routine use of cell monolayers cultivated in multi-well plates. This configuration fails to recapitulate the complex architecture of vascular networks *in vivo* and does not capture the relationship between shear stress (i.e. flow) experienced by the cells and dose of the applied pharmacological agents. Microfluidic platforms have been applied extensively to create vascular systems *in vitro*; however, they rely on bulky external hardware to operate, which hinders the wide application of microfluidic chips by non-microfluidic experts. Here, we have developed a standalone perfusion platform where multiple devices were perfused at a time with a single miniaturized peristaltic pump. Using the platform, multiple micro-vessel networks, that contained three levels of branching structures, were created by culturing endothelial cells within circular micro-channel networks mimicking the geometrical configuration of natural blood vessels. To demonstrate the feasibility of our platform for drug testing and validation assays, a drug induced nitric oxide assay was performed on the engineered micro-vessel network using a panel of vaso-active drugs (acetylcholine, phenylephrine, atorvastatin, and sildenafil), showing both flow and drug dose dependent responses. The interactive effects between flow and drug dose for sildenafil could not be captured by a simple straight rectangular channel coated with endothelial cells, but it was captured in a more physiological branching circular network. A monocyte adhesion assay was also demonstrated with and without stimulation by an inflammatory cytokine, tumor necrosis factor- α .
© 2013 AIP Publishing LLC. [<http://dx.doi.org/10.1063/1.4818837>]

INTRODUCTION

Our ability to study drug efficacy and toxicity *in vitro* under conditions predictive of actual human physiology depends on the development of systematic approaches to generate realistic experimental models. Such models can provide valuable information under highly controlled and multiplexed conditions thereby serving as cost-effective alternatives to animal testing. In recent years, microfluidic technologies have made significant progress in generating complex *in vitro* models to recapitulate organ level function of liver,¹ lung,² and heart,³ which would otherwise be unattainable with conventional macro-scale systems. However, to better understand the effects of organ-organ level interactions, metabolic/oxygen gradients, and cellular

^{a)} Author to whom correspondence should be addressed. Electronic mail: m.radisic@utoronto.ca. Telephone: 416-946-5295. Fax: 416-978-4317.

trafficking through different tissues, a vascular circulatory system is a crucial component to bridge multiple organ models into an integrated physiological system. The vascular circulatory system would not only facilitate the transport of molecular and physical regulatory factors between different tissues but also carry out its own regulatory functions in responding to hemodynamic shear stress, circulating cytokines, blood-endothelium interactions, and spatial structural cues.

Studying the effects of pharmacological agents on human endothelium includes the routine use of cell monolayers cultivated in multi-well plates. This configuration fails to recapitulate the complex architecture of the *in vivo* vascular networks and does not capture relationships between shear stress (i.e., flow) experienced by the cells and dose of the applied pharmacological agent. Therefore developing an *in vitro* vascular system that can recapitulate these factors and permit efficient and systematic experimentation is an important step towards the development of integrated human physiological models for drug target validation.

Macro-scale parallel plate flow systems⁴ have been used extensively to study the effect of hemodynamic shear stress on endothelial cells, but this approach is not a viable option for integration with microfluidic systems and high throughput experimentation, nor does it provide realistic spatial arrangement of endothelial cells mimicking the physiological tubular structure of micro-vessels. Current microfluidic approaches either culture endothelial cells simply on the bottom of a micro-channel^{5–7} or coat endothelial cells around a rectangular channel with sharp corners.^{6–10} These approaches can establish a vasculature quickly in defined conditions but ignore the artifacts generated by the sharp corners on the endothelialized lumen. Although remodeling of collagen gels allows for formation of circular lumens, fragility of these gels limits the complexity of branching structures and levels of branching, enabling creation of structures that branch only to the first order,⁶ in contrast to the native vasculature that follows fractal rules in branching. Other approaches allow the endothelial cells to sprout into a hydrogel compartment on-chip thus generating more natural micro-capillaries.¹¹ Although these micro-capillaries are more physiological, their overall branched structure is difficult to control and takes up to 4 days to establish.

Our goal here was to develop a standalone endothelial culture/assay system that can be established rapidly (e.g., overnight) and that includes multiple endothelialized branched circular micro-channel networks in parallel, with each network containing multiple levels of branching similar to the native vasculature. Furthermore, to demonstrate the feasibility of our platform for drug testing and validation assays, induced nitric oxide secretion of the micro-vessel network was analyzed upon stimulation by a panel of four drugs, acetylcholine, phenylephrine, atorvastatin, and sildenafil under flow conditions, using conventional monolayers on tissue culture plates as a control. We hypothesized that developing high-fidelity models of the native vasculature *in vitro* will enable us to capture complex interactions between flow conditions and applied pharmaceutical agent concentrations that are often missed in other more simplified configurations. The developed system was perfused by a portable peristaltic pump that operated above 1 $\mu\text{l}/\text{min}$. The entire platform, which was comparable in size to standard 96 well plates, required only an external electric plug to operate, it fit comfortably inside a standard incubator and reduced reagent consumption to only 200 μl of drug solution per assay, a critical criterion for validation of expensive pharmaceutical agents.

MATERIALS AND METHODS

Miniaturized pump fabrication

The permanent part of the pump includes a small motor (Creatron Inc., 6 V Gearmotor, 70 mA free-run, 1.6 A stall, 40 oz-in(2.9 kg-cm)) connected to an elliptically shaped metal shaft. The exchangeable part of the pump includes a PDMS block embedded with micro-Tygon tubing (250 μm inner diameter, 750 μm outer diameter) wrapped around a through hole that matches the size of the shaft. This piece was fabricated by wrapping multiple tubes in parallel around a needle with 2.5 mm outer diameter and then embedding the needle in polydimethylsiloxane (PDMS) similar to a previous design.¹² The needle was later removed leaving behind

a through hole for the insertion of the shaft. The shaft had an elliptical cross section of approximately 1 mm by 3 mm. When the shaft was inserted into the hole, it compressed the microtubes wrapped around the hole at two points opposite of each other (Figure 1(b)(ii)). As the shaft turned, it continuously squeezed the tube and drove a consistent amount of fluid within the tube forward with each turn as shown in Figure 1(b)(iii). In our design, we have incorporated four parallel tubes within a single pump and used it to perfuse four separate microfluidic devices at a time (Figure 1(a)). The output flow rate could be adjusted by the inner diameter of the tubing used as well as by the rotational speed of the shaft, which was controlled by the applied voltage to the pump.

Microfluidic device fabrication

The microfluidic device included four branching networks connected in parallel. Each branching network included two 400 μm channels that branched into four 200 μm channels and then into eight 100 μm channels (Figure 1(b)(iv)). The channel height of the network was 100 μm . Each branched network had inner luminal surface area of 0.34 cm^2 closely matching the surface area (0.31 cm^2) of an individual well in a 96 well plates. The device was fabricated via standard soft lithography techniques as described previously.¹³ Briefly, silicon wafer was coated with SU-8 photoresist. The SU-8 photoresist was exposed to 365 nm, 11 mW/cm^2 UV light through a transparency mask, using a mask aligner (Q2001, Quintel Co., San Jose, CA). The unexposed photoresist was removed with SU-8 developer. Silicone elastomer [poly(dimethylsiloxane), PDMS] and curing agent (10:1 ratio) were mixed and molded to the SU-8 masters at 75 $^{\circ}\text{C}$ for 1 h. The replicas were plasma treated and bonded to another flat PDMS.

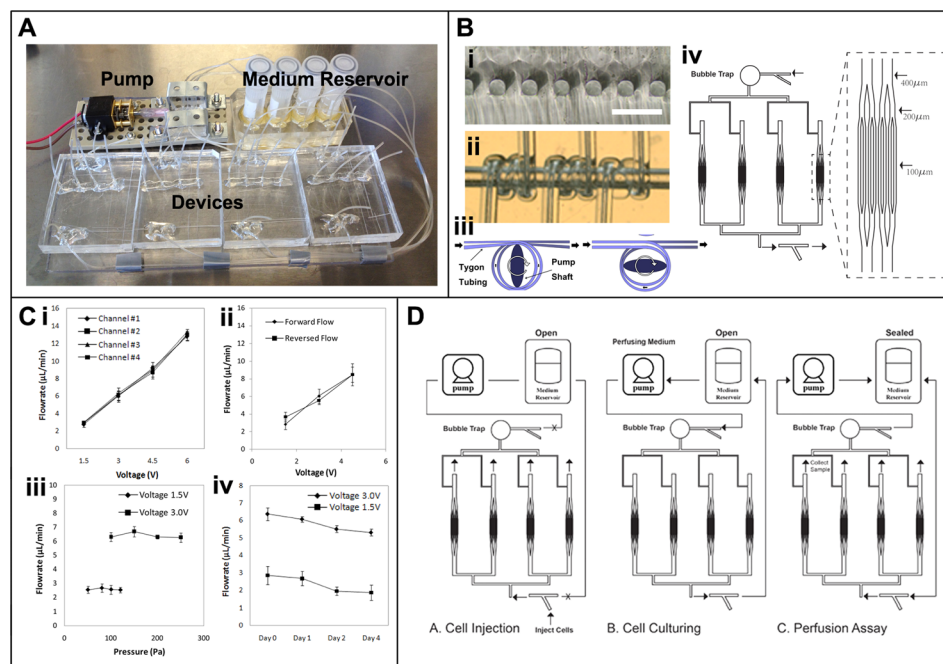


FIG. 1. System setup and characterization. (a) Image of the standalone culturing/assay platform. (b)(i) Cross sectional view of the circular micro-channels. Scale bar, 300 μm . (b)(ii) Magnified view of the tubing coil within the PDMS block. (b)(iii) Schematic illustrating the turning of the pump shaft as it locally compressed the tubing and drove the fluid flow. (b)(iv) Microfluidic device schematic illustrating the dimension of the branched network as well as the overall parallel configuration of the four branching networks on a single device. (c)(i) Flow rate measurement of the four independent flow circuits through the four microfluidic devices, $n = 3$. (c)(ii) Flow rate measurement of the miniaturized pump determined via PIV in both forward and reversed flow direction. (c)(iii) Pump stability under various pressures, $n = 3$. (c)(iv) Stability of the pump over 4 day period, $n = 3$. (d) Schematic of the device operation for cell injection, cell culturing, and perfusion assay.

Bubble trap fabrication

To prevent bubbles from reaching the cells, a simple bubble trap was placed upstream of the cell culture area to trap any bubbles that entered the device¹⁴ (Figure 1(b)(iv)). The bubble trap was fabricated by carving out a conical shaped well in the PDMS device upstream from the micro-vessel network, hence trapping all bubbles before they reached the cells.

Air injection molding

Fabricated PDMS channels initially had rectangular cross sections with sharp corners. To mimic the geometrical configuration of natural blood vessels, the channels were modified via air injection to yield a circular cross section as demonstrated previously.¹⁵ Briefly, PDMS pre-polymer solution was first injected to fill the channel network. Then, vacuum was applied at the outlet to pull the PDMS back through the outlet while at the same time baking the device on hot plate at 200 °C to quickly polymerize the residual PDMS. Constant airflow through the network kept all the channels open while residual PDMS rapidly polymerized at the corner of the channel and left behind circular cross sections as shown in Figure 1(b)(i). To create the control straight rectangular channel, no air injection molding was applied. Fabricated open channels were simply closed by plasma bonding to another flat PDMS sheet.

Perfusion cultivation and drug testing

The medium reservoir was created by cutting off the bottom of a 2 ml Eppendorf vials and embedding them on top of microfluidic channels. By connecting the pump, reservoir, and the microfluidic device together in a closed loop flow circuit, a perfusion platform was created where culture medium was recycled over time. The flow circuit was always primed with 100% ethanol and then sterilized with 70% ethanol. After sterilization, the micro-channels were also coated with gelatin by incubating the channels with 0.2% gelatin solution, which was sufficient to allow cell attachment. These procedures could be simply carried out with the built-in pump and by changing the solution in the reservoir. To inject cells into the microfluidic device, connections to the pump and reservoir were clamped shut leaving one cell injection inlet and four outlets open on the device. Endothelial cell suspension (100–200 μ l) at a high concentration (30×10^6 cells/ml) was injected from the cell injection inlet to evenly fill the networks with the cells. (Figure 1(d)) Seeded cells were then left to attach at static conditions for 2 h at 37 °C with 5%CO₂. Unattached cells were then flushed out of the network by starting the perfusion. The endothelial networks were cultivated under perfusion and re-circulation of the culture medium by the pump at the flow rate of 6 μ l/min with applied voltage of 3 V corresponding to a wall shear stress of 0.56 dyn/cm² and Reynolds number of 0.089. The cap of the medium reservoir was left loose for gas exchange. Cells were cultured under continuous perfusion for 2–4 days. Drug assays and monocyte adhesion assays were performed by replacing the culture medium in the medium reservoir with the corresponding drug solution or monocyte cell suspension. During long-term cell-culture, the medium was perfused from the pump to the bubble trap to the vessel network to eliminate any bubbles before the culture medium reached the vessel network. However, the bubble trap had large dead volume causing a time delay in introduction of new solutions. Therefore, drug solutions were perfused from the reservoir to the vessel network then to the pump in reverse to avoid the bubble trap hence preventing drug dilution (Figure 1(d)). Since drug stimulation occurred in a short period of time, bubble formation within the flow circuit was usually not an issue.

Endothelial cell culture

Human umbilical vein endothelial cells (HUVECs) were purchased from Lonza and cultured with endothelial growth medium (EGM, Lonza). Only passage 3–5 HUVECs were used for experiments. HUVEC were cultured in 96 well plates for two days until confluent. The cells

were then trypsinized and seeded into microfluidic devices for perfusion cultivation as described above. For drug testing purposes, static controls were kept in 96 well plates.

Immunofluorescent staining

Immunofluorescent staining was performed to assess the micro-vessel networks. The micro-vessel networks were first fixed in 4% (w/v) paraformaldehyde in phosphate buffered saline (PBS) for 15 min at room temperature. The cells were then blocked using 5% fetal bovine serum (FBS) in PBS for 1 hour and permeated with 0.25% Triton X100 in PBS. Next, the micro-vessels were incubated with one of the primary antibodies CD31, von Willebrand factor, VE-cadherin, or Ki-67 (Mouse, 1:200 dilution, Sigma) overnight at 4 °C. The micro-vessels were then incubated with an appropriate secondary antibody, Alexa 488 conjugated anti-mouse IgG (1:200 dilutions, Sigma) and/or TRITC conjugated anti-rabbit IgG (1:200 dilution, Sigma) for 1 h. Finally the micro-vessels were imaged with a confocal microscope (Olympus FV5-PSU confocal with IX70 microscope).

Pump performance characterization

The output flow rates from the pump were determined by measuring both the fluid volumetric flow rate at the device outlet as well as mapping the flow velocity of micro-particles (1 μm) within the micro-channels with particle image velocimetry (PIV). The rotation speed of the pump shaft was controlled by an external voltage adaptor with varying voltage inputs of 1.5 V, 3 V, 4.5 V, and 6 V. To characterize the performance of the pump under varying pressures or resistances, the pump outlet was connected to micro-tubes (300 μm inner diameter) with various lengths (from 200 cm to 500 cm) to generate various resistances. These resistances were then converted into pressure based on the corresponding flow rate indicating the pressure applied to the pump during pumping. To calculate the pressure applied on the pump under various resistances created with the micro-tubing, the following was applied:

$$\Delta P = \frac{8\mu L Q}{\pi r^4}. \quad (1)$$

Laminar flow was assumed since the Reynolds number was below 2300 in all the experimental conditions.

Cell alignment analysis

Cell orientation at different locations of the vascular network was characterized by the orientation of the nuclear staining (DAPI). Images were analyzed using MATLAB image processing tools. The extent of overall cell alignment was quantified with standard deviation square (σ^2) of the cell orientation angle distribution.

Drug solution preparation

Drugs (atorvastatin, cat# PZ0001, sildenafil, cat# PZ0003, phenylephrine hydrochloride, cat# P6126, and acetylcholine chloride, cat# A2661) were purchased from Sigma in powder form. All drugs were first dissolved in DMSO and then diluted to the indicated concentration in phenol-red free Dulbecco's modified Eagle's medium (DMEM) with 0.5% FBS supplemented with 100 μM L-arginine (Sigma). The concentration of DMSO was kept lower than 0.5% of the final solution in all conditions.

Nitric oxide assay

After 2 days of culturing, the branched circular micro-vessel networks and endothelial monolayer cultured under static conditions were stimulated with various drug solutions. First, the micro-vessels were rinsed with PBS by pumping fresh PBS through the network. Then,

drug solutions supplemented with 100 μ M L-arginine were added individually into each reservoir. The solution was then perfused through the micro-vessels at 2.5 μ l/min for 1.5 h while collecting the output solution at the four outlets. The collected solution was then quantified for nitrite concentration with a quantitative fluorometric extracellular nitric oxide assay (Calbiochem). Since the final products of nitric oxide are nitrates and nitrites, this assay uses nitrate reductase to convert nitrates to nitrites and then uses 2,3-diaminaphthalene and NaOH to convert nitrites to a fluorescent compound. Plates were read using a Wallac 1420 Multilabel Victor microplate reader (Perkin Elmer), with excitation at 355 nm and emission at 430 nm. If the interactive effect between flow rate and drug dose for a given drug was observed in branched circular network vs. static 96-well plate, a straight rectangular channel perfusion was added as an additional control.

Monocyte adhesion assay

Prior to the experiment, the micro-vessel networks were treated with 25 ng/ml TNF- α (Invitrogen) in EGM medium under perfusion for 4 h with TNF- α free networks used as controls. RAW264.7 cells (ATCC, Manassas, VA) were maintained in DMEM with 10% FBS and 1% penicillin/streptomycin. Only passage 3–6 RAW264.7 cells were used for the experiment. Prior to the experiment, RAW264.7 cells were fluorescently labeled with calcein AM (Invitrogen) and resuspended at a concentration of 10^6 cells/ml. Monocyte cell suspension (1 ml) was placed within each reservoir and perfused through the micro-vessel network at 2.5 μ l/min for 1 h. The cell suspension within each reservoir was agitated occasionally to prevent cell settlement. Unattached cells were washed away with fresh PBS after 1 h. Two images were taken along the micro-vessels for each micro-vessel network with inverted fluorescent microscope (Olympus). The number of adherent cells in each image was quantified with IMAGEJ software and averaged for each device. Four micro-vessel networks were tested per group.

Statistical analysis

Error bars in figures represent standard deviation. Statistical significance was determined using Student's t-test and Two-Way ANOVA. $p < 0.05$ was considered significant. A minimum of 3 samples were used per data point. For data collected from nitric oxide assay, two factor ANOVA test was performed with 3 data points in the perfusion condition and 3 representative data points (out of the 6) in the static culture control because the two-way ANOVA tests require all groups to contain same number of repeats. Standard deviation for the static culture control was derived from the 6 data points.

RESULTS AND DISCUSSION

Miniaturized peristaltic pump and the network structure

On our platform, four devices were perfused at a time in parallel with a single pump (Figure 1(a)). Within each microfluidic device, four networks were placed in parallel and perfused with a single inlet as shown in Figure 1(b)(iv), therefore leading to perfusion of 16 micro-vascular networks on each platform. The microvascular network was made up of a hierarchy of bifurcation branches starting from two 400 μ m channels which branched into four 200 μ m channels and then into eight 100 μ m channels. The microchannels within the branched network also had circular cross sections mimicking the circular spatial configuration of natural blood vessels as shown in Figure 1(b)(i).

The developed miniaturized pump contained a permanent component including a motor and a shaft as well as an exchangeable component, a PDMS block embedded with flexible micro-tubing (Figure 1(b)(ii, iii)). The exchangeable component is simple to fabricate and can incorporate multiple pieces of tubing to drive multiple devices in parallel with a single pump. The output flow rates from the pump at various applied voltages were determined by measuring the fluid output at the tubing outlets of the pump. The correlation between the applied voltages

and generated flow rates was determined and shown in Figure 1(c)(i,ii). Within the tested applied voltage, in the range from 1.5 V to 6 V, there was a linear relationship between the voltage and the generated flow rate which ranged from 2 $\mu\text{l}/\text{min}$ to 14 $\mu\text{l}/\text{min}$ corresponding to a wall shear stress in the range from 0.2 to 1.3 dyn/cm^2 and Reynolds number in the range from 0.03 to 0.2 within the micro-channels.

These measurements were verified with particle image velocimetry (PIV) by measuring the micro-particle flow velocity within the micro-channels (Figure 1(c)(ii)). No significant differences between the two methods were found. The flow direction was also reversed by rotating the pump shaft in a reverse direction and generated flow rates were not significantly different. The flow rate range was chosen to generate a range of wall shear stresses matching those within venules, although higher shear stress might be required if other arterial conditions are to be tested.

Multiple tubing pieces were incorporated with a single pump to demonstrate parallelization. The flow rate generated by different pieces of tubing closely matched each other, as shown by the closely overlapping data points in Figure 1(c)(i), demonstrating the consistency of this device in generating flow rates across multiple flow circuits in parallel. The performance of the pump over time was also examined (Figure 1(c)(iv)) at two different applied voltages (1.5 V, 3 V). The pump performance appears to drop gradually over a 4-day period for some conditions due to the tear-and-wear on the tubing. There was a statistically significant difference in the generated flow rates between day 4 and day 1 for 3 V but not for 1.5 V, indicating that conditions which enable maintenance of pump function over at least 4 days in culture can be found. Additionally, the tubes and the PDMS block are the replaceable parts of the pump and therefore can be replaced for each new experiment. Finally, the stability of the pump under various pressures or resistances was considered (Figure 1(c)(iii)). The performance of the pump was found to be consistent under the tested pressure ranges. This test demonstrated that the pump could operate at the pre-determined flow rate without being affected by varying resistances in the flow circuit.

Engineered micro-vessel network

Micro-vessel networks were created by cultivating HUVECs seeded at a high cell concentration on the inner lumen of the pre-fabricated circular micro-channel networks (Figure 1(d)). Seeded endothelial cells were able to attach, proliferate, and cover the entire luminal surface forming a micro-vessel network with pre-defined branching vessel structure within 2 days. On day 2, the micro-vessel network was fixed and stained with CD31, VE-cadherin, and von Willebrand factor (VWF) (Figure 2(a)). The expression of CD31 and VE-cadherin at the cell-cell interface outlined the endothelial morphology and confirmed the formation of inter-cellular junctions (Figure 2(a)(i-vii)). However, small voids between endothelial cells were also observed as indicated by the white arrows (Figure 2(a)(ii,iii)). Huynh and co-workers¹⁶ have shown that intimal stiffening *in vivo* and stiff substrates *in vitro* could disrupt endothelial cell-cell junction integrity leading to increased permeability. Therefore, the use of a stiff substrate such as PDMS could have a destabilizing effect on the endothelial junctions, which could explain the presence of small void spaces in cell-cell junctions. The cross-sectional view of the micro-vessel demonstrated that endothelial cells covered the inner luminal surface of the micro-channels after 2 days. The expression of von Willebrand factor on the endothelial cells is also shown in Figure 2(a)(viii-x)).

Circular channels not only help create more realistic vessel geometrical configuration, in practice their advantage compared to the rectangular channels became obvious when the engineered vessels were cultured for longer than 4 days as shown in Figure 2(a)(xi-xii). The endothelial coating within the rectangular channels gradually detached from the channel walls at the four sharp corners, possibly due to increasing intercellular tension and decreasing cell adhesion to PDMS surface. The presence of areas with high tension at the corners of rectangular channels, which are often neglected in other configurations,⁸ may result in non-physiological cell responses. In contrast, endothelial coating within circular channels remained stably attached.

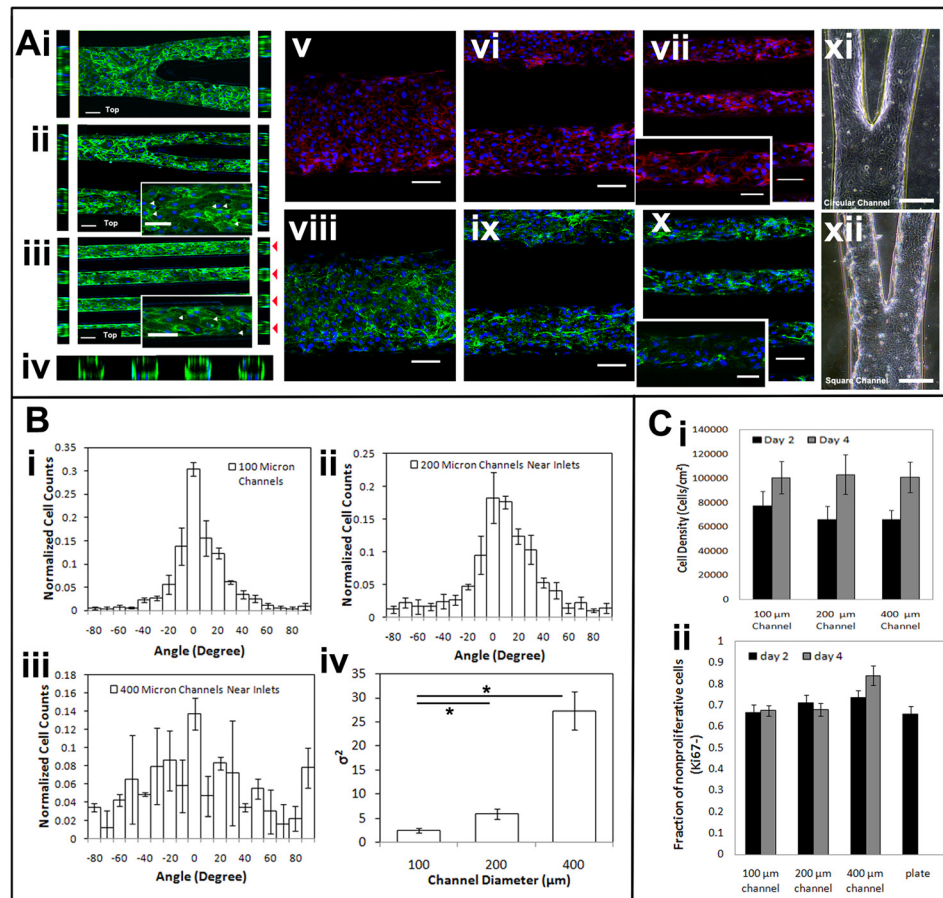


FIG. 2. Immunofluorescence staining of the micro-vessel network. (a) Top view (middle) and cross sectional view of the circular channels (sides) in the micro-vessel network at (i) 400 μm segment, (ii) 200 μm segment, (iii) 100 μm segment, and (iv) cross section. Scale bar, 100 μm CD31-green, DAPI-blue. White arrows indicate void space between cells. Red arrows indicate the cross section of the 100 μm micro-vessels. (a(v-vii)) Top view of the micro-vessel network with VE-cadherin staining-red, DAPI-blue, Scale bar, 100 μm . Inset scale bar, 50 μm . (a(viii-x)) Top view of the micro-vessel network with von Willebrand factor staining-green. Scale bar, 100 μm . Inset scale bar, 50 μm . (a(xi-xii)) Brightfield image of a branched section of endothelialized network in circular and rectangular channel, respectively. (b(i-iv)) Cell orientation characterization, $n = 3$. (C(i)) Quantification of cell density at day 2 and 4 within the vessel network, $n = 3$. (C(ii)) Quantification of the Ki67 positive staining at day 2 and 4, $n = 3$.

The orientation of the endothelial cells within the micro-vessel network was characterized based on the alignment of the cell nucleus and grouped based on their location within the network as shown in Figure 2(b(i-iii)). Cells located within the 100 μm segments, 200 μm segments, and 400 μm segments of the micro-vessel network as shown in Figure 2(a(i-iii)) were grouped separately and characterized based on their orientation with respect to the micro-channel side walls. *In vitro*, we found cells were more likely to align along the micro-channels in the narrower channels while cells were more randomly oriented in the larger channels. The behaviour of cells in narrower channels is consistent with the *in vivo* observations where endothelial cells are elongated and aligned in arterioles in venules.¹⁷ As shown in Figure 2(b(iv)), there was a significant difference in cell alignment between the 100 μm group and the 400 μm group. Since the bifurcation network was designed so that the cells within the channel network all experienced similar fluid shear stress, this indicated that the presence of spatial confinement had an effect on the cell morphology rather than the shear stress. Different from topographical features applied in 2-D cell culture where cells sense sharp geometrical features that guide their alignment, within our circular micro-vessel network, the cells, wrapping around the entire lumen, do not sense any sharp edges of the channel, instead they are guided solely by the

spatial constriction. This indicates that cell directionality can be influenced by spatial confinement alone, decoupled from topographical guidance. On the other hand, as reported by Zheng *et al.*⁶ when endothelial cells are confined within soft material (e.g., Type I collagen gel), they do not show any net alignment suggesting that substrate stiffness could also have a profound influence on the observed guidance phenomenon on PDMS substrate. In future studies, polymeric substrates that better recapitulate mechanical stiffness of the native vasculature than PDMS will be developed and used for engineering of a branching vascular network.

To assess the quiescent state of the micro-vessel network, Ki67 marker was used to mark the proliferative cells. On day 2, 30% of the cell population was positive for Ki67, which indicated that many cells were still proliferating (Figure 2(c)(ii)). The overall percentage of proliferating cells did not change significantly at day 4. There were no significant differences between cells located within different network segments. Due to cell proliferation, cell density within the micro-vessel network increased from day 2 to day 4 (Figure 2(c)(i)). The presence of proliferative cells could be caused by the presence of small void spaces within the endothelial layer, which signaled the endothelial cells to proliferate continuously.

Drug induced nitric oxide secretion and monocyte adhesion

To demonstrate the applicability of the platform for *in vitro* drug screening, four drugs (acetylcholine, phenylephrine, atorvastatin, and sildenafil) were examined and their effects on the secretion of nitric oxide from endothelial cells were characterized. Acetylcholine is known for its function on stimulating intracellular nitric oxide production and release in endothelial cells during blood vessel relaxation,^{18,19} thus it was used as a positive control. Phenylephrine is known for its effect on smooth muscle cells in inducing vessel constriction and lack of an effect on endothelial cells, thus it was used as a negative control.²⁰ Atorvastatin is a drug commonly used to control high blood lipids levels, especially in patients with diabetes. It has been shown in some studies to regulate nitric oxide synthase in cardiac function, but its direct effects on endothelial cells are not clearly delineated and depend strongly on the type of animal model (e.g., diabetic vs. non-diabetic) and specific tissue investigated.²¹ While some studies failed to report restoration of vascular dysfunction after atorvastatin treatment in diabetic patients, other animal studies indicated improvements in endothelial function in a tissue specific manner.²² Lastly, sildenafil has been shown to cause vessel dilation by inhibiting cGMP-specific phosphodiesterase type 5, which degrades cGMP and hence results in elevated level of cGMP that leads to smooth muscle relaxation, thus its effects on vessel relaxation were not expected to be endothelial specific.²³ However, in a recent study, sildenafil was also reported to increase expression of nitric oxide synthase in human endothelial cells²⁴ motivating the study of sildenafil here.

Engineered micro-vessel networks were stimulated with the four drugs and the accumulation of nitrite within the collected culture medium was analyzed (Figure 3(a) and 3(c)(i–iv)). Endothelial cells cultured in 96 well plates were used as static control. It is not possible to culture endothelial cells within micro-channel networks for several days without medium perfusion, due to the limitations in medium and oxygen supply in a closed system. Thus, the media would have to be changed at least intermittently which would generate shear stress and therefore would not represent a good static control. We also wanted the static control to represent a system that is currently most often used in drug testing and physiological studies on endothelial cells, and that is a 96-well plate.

In the engineered vessel network, drug absorption onto the PDMS wall should be minimal, since the channels were fully coated with endothelial cells and the duration of the experiment was short. The Péclet number for the experimental condition was as high as 200 for the smallest drug molecule (acetylcholine), indicating fluidic convection dominated molecular diffusion, further arguing for a sufficient drug supply to the channel. A range of drug doses (10 μ M to 1 mM) was tested on this platform to screen the response of the cells over a large range of drug concentrations. For instance, small molecules, such as acetylcholine, are usually released by cells through cell signalling and could generate high local concentrations *in vivo*. Studies have shown the contraction response of isolated arteries to acetylcholine stimulation at dose range

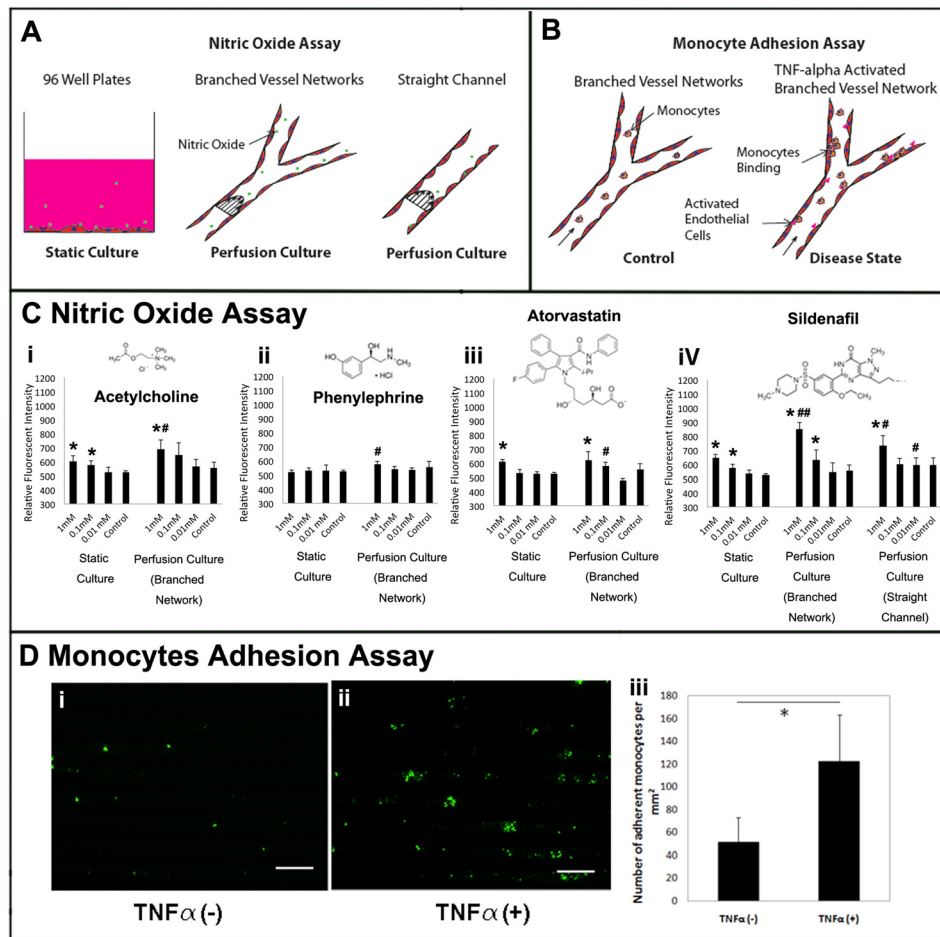


FIG. 3. Drug induced nitric oxide and monocyte adhesion assay. (a) Schematic of the experimental conditions of the nitric oxide assay. (b) Schematic of the experimental conditions of the monocytes adhesion assay. (c (i–iv)) Nitric oxide in static culture ($n = 6$) and perfusion culture in both branched circular channels and rectangular straight channels ($n = 3$) with quantitative fluorometric extracellular nitric oxide assay. * indicates a significant difference compared to the drug-free control at the same culture condition with $p < 0.05$. # indicates a significant difference in comparison to the corresponding static culture condition with $p < 0.05$. ## indicates significant additive interaction between culture conditions and drug concentrations. (d(i,ii)) Representative images of adherent monocytes within the micro-vessel network. Monocytes were labeled green. Scale bar, 300 μm . (d(iii)) Quantification of adherent monocytes density within micro-vessel networks, $n = 3$.

from 1 μM to 10 μM (Ref. 20) while others have tested the effect of acetylcholine at up to 1 mM for HUVECs *in vitro*.²⁵ Typical pharmaceutical drugs, such as sildenafil, are orally administered and dissolve into blood reaching concentration above 1 μM .²⁶ Other studies have tested sildenafil *in vitro* at 10 μM on primary cardiac cells²⁷ to 0.1 mM on isolated arteries.²⁸ On our platform, pronounced responses were seen at 0.1 mM concentration. Higher drug dosage appears to be critical in generating robust cell response over a short stimulation period (1.5 h).

As expected, nitric oxide secretion was elevated upon stimulation with acetylcholine and showed no significant changes upon stimulation with phenylephrine in both static (96-well plates) and perfusion culture. Nitric oxide level upon stimulation by acetylcholine also showed a significant increase in perfusion culture compared to the static culture at the drug concentration of 1 mM. Furthermore, both atorvastatin and sildenafil appeared to induce nitric oxide secretion in static culture, while only sildenafil induced significant increase in nitric oxide secretion in perfusion culture compared to the drug-free control.

The perfusion culture resulted in a higher nitric oxide release upon application of higher doses of drugs for acetylcholine, atorvastatin, and sildenafil compared to the static culture, emphasizing the importance of drug validation under physiologically realistic endothelial cell

geometry and flow rates. This effect was especially profound for sildenafil at the drug concentration of 1 mM demonstrating an additive interactive effect of flow and drug concentration on drug induced endothelial function.

Since the interactive effect of flow and drug concentration was observed for sildenafil in the branched microvessel network, we wanted to determine if a similar effect could be captured by a commonly used rectangular channel coated with endothelial cells and cultivated under perfusion. In the rectangular channel, no significant additive effect between flow and drug concentration was observed for sildenafil suggesting that branched circular channel network could be a more realistic platform for probing endothelial drugs (Figure 3(c)(iv)). Higher nitric oxide concentrations upon 1 mM sildenafil treatment were observed in the branched network, in comparison to either static culture or a rectangular perfused channel (Figure 3(c)(iv), demonstrating that simplified geometrical configurations may underestimate the effect of this drug on endothelial cells. Uniform fluid flow and wall shear stress on the endothelial lumen could contribute to the more pronounced interaction between flow and drug concentration in the circular branched channel network. Our findings illustrate that reproducing physiological complexity *in vitro*, enables us to capture higher-order interactions that are often missed in simplified geometries (e.g., a straight rectangular channel).

The additive interaction between flow and drug concentration was seen with sildenafil but not acetylcholine. It is known that both flow and acetylcholine induce the production and secretion of nitric oxide by increasing the presence of nitric oxide synthase through the same nitric oxide signalling pathway, thus, the pathway may already be at saturation and no further increase might be possible. Sildenafil on the other hand have been shown to stimulate nitric oxide not only through nitric oxide synthase but also by stabilizing cGMP, which consequently promotes the accumulation of nitric oxide through the nitric oxide-guanylate cyclase pathway.²⁹ This alternative signal pathway would allow sildenafil to escalate the presence of nitric oxide in addition to flow-induced stimulation. Previously, the additive effect of drug application and shear flow was reported in other systems. Wang *et al.*³⁰ demonstrated that the effect of combretastatin A-4 can be significantly enhanced under shear flow condition above 2 dynes/cm². In our study, the additive effect of fluid flow in conjunction with drug dosing was manifested even at a shear stress below 1 dynes/cm². Increasing applied shear stress could lead to even more pronounced effects, however, we focused at the levels of shear stress relevant in microcirculation. Fluid shear induced nitric oxide secretion in endothelial cells has been shown within micro-channels by using nitric oxide micro-detector to track the nitric oxide level in a single channel in real time.³¹ The use of the highly sensitive detector allowed the detection of even slightly elevated nitric oxide levels with increasing shear forces from 0.08 dynes/cm² to 0.65 dynes/cm². Although the use of such detectors improved sensitivity, the ability to multiplex was lost. In our platform, 16 branched networks can be screened at a time at varying drug concentrations.

To demonstrate the applicability of the platform for investigating monocyte-endothelial cell interaction, monocytes were perfused through the micro-vessels under both healthy state and diseased state stimulated by an inflammatory stimulus, tumor necrosis factor- α (TNF- α) (Figure 3(b)). Exposure to TNF- α is known to increase surface adhesion proteins of endothelial cells, such as vascular cell adhesion molecules-1 (VCAM-1), that recruit and bind to monocytes. This inflammatory condition is relevant for the study of immune response to injury and variety of diseases. Therefore recapitulating this interaction *in vitro* could help probe the effectiveness of drugs in suppressing vascular inflammation. With stimulation, monocyte attachment on the micro-vessel network increased dramatically from the healthy control suggesting the micro-vessel network can capture the effect of the stimuli, promoting monocyte attachment (Figure 3(d)). In addition, in both stimulated and non-stimulated micro-vessels, the density of the adherent monocytes (50 cells/mm² and 120 cells/mm², respectively) was approximately 40% lower than previously reported on an endothelial cell monolayer under flow condition,⁵ which may suggest that the presence of curvature wall and geometrical confinement could affect flow path and cell-cell binding. Therefore the circular micro-channels could be a more realistic and improved model compared to the overly simplified parallel plate bioreactor and rectangular micro-channels.

Overall, the advantages of the developed system over those previously described are that we can create fully endothelialized circular micro-vascular structures with at least 3 levels of branching that can capture complex interactions between the flow and applied drug dose which could not be captured by more simplified rectangular channels. Previously developed systems relied on the use of rectangular channels with only one order of branching⁹ or membrane microfluidic devices where monolayers of endothelial cells were cultivated.⁵ Although more complex devices were envisioned in a mathematical modeling study focusing on designing networks that minimize vascular volume fraction, no designs were experimentally implemented and seeded with cells.¹⁰ Although biologists may not be willing to fabricate the platform on their own, the platform contains all the components required for its operation. Thus, it could be easily packaged along with the microfluidic chips in a way that does not require assembly and delivered directly to the end user as an off-the-shelf product, thus facilitating technology adoption. For high-throughput pharmaceutical testing, the chip platform could be made more robust if combined with robot liquid handlers.

CONCLUSIONS

We have demonstrated a standalone platform for culturing multiple micro-vessel networks in parallel for drug induced nitric oxide and monocyte adhesion assay. Multiple different drug solutions or cell suspensions can be perfused through each micro-vessel network at a time by using a single pump hence performing multiple assays in a single run. The compact setup minimizes total drug consumption and allows recirculation of cell medium during culture. The platform also provides additional geometric features by the use of pre-fabricated circular micro-channels mimicking the geometrical configuration of natural blood vessels, which is not available on standard multi-well plates. Engineered micro-vessel network was shown to promote cell alignment within narrower channels even under low shear stress condition suggesting the role of spatial confinement in guiding cell morphology. The standalone platform greatly simplified the setup for perfusion based cell culture as well as flow based assays within the microfluidic devices by eliminating bulky external equipment. The entire platform can be easily stored within incubators for cell culture as well as placed under a microscope for imaging, all while applying constant flow through the micro-vessel networks.

ACKNOWLEDGMENTS

This work has been funded in part by Grant No. R01 EB009327 from the National Institute of Health (NIH) of the U.S. Department of Health & Human Services.

- ¹K. Domansky, W. Inman, J. Serdy, A. Dash, M. H. M. Lim *et al.*, "Perfused multiwell plate for 3D liver tissue engineering," *Lab Chip* **10**, 51–58 (2010).
- ²D. Huh, B. D. Matthews, A. Mammoto, M. Montoya-Zavala, H. Y. Hsin *et al.*, "Reconstituting organ-level lung functions on a chip," *Science* **328**, 1662–1668 (2010).
- ³A. Grosberg, P. W. Alford, M. L. McCain, and K. K. Parker, "Ensembles of engineered cardiac tissues for physiological and pharmacological study: Heart on a chip," *Lab Chip* **11**, 4165–4173 (2011).
- ⁴J. A. Frangos, L. V. McIntire, and S. G. Eskin, "Shear stress induced stimulation of mammalian cell metabolism," *Biotechnol. Bioeng.* **32**, 1053–1060 (1988).
- ⁵S. Srigunapalan, C. Lam, A. R. Wheeler, and C. A. Simmons, "A microfluidic membrane device to mimic critical components of the vascular microenvironment," *Biomicrofluidics* **5**, 13409 (2011).
- ⁶Y. Zheng, J. Chen, M. Craven, N. W. Choi, S. Totorica *et al.*, "In vitro microvessels for the study of angiogenesis and thrombosis," *Proc. Natl. Acad. Sci. U.S.A.* **109**, 9342–9347 (2012).
- ⁷M. Y. Rotenberg, E. Ruvinov, A. Armoza, and S. Cohen, "A multi-shear perfusion bioreactor for investigating shear stress effects in endothelial cell constructs," *Lab Chip* **12**, 2696–2703 (2012).
- ⁸M. Tsai, A. Kita, J. Leach, R. Rounsevell, J. N. Huang *et al.*, "In vitro modeling of the microvascular occlusion and thrombosis that occur in hematologic diseases using microfluidic technology," *J. Clin. Invest.* **122**, 408–418 (2012).
- ⁹L. T. Chau, B. E. Rolfe, and J. J. Cooper-White, "A microdevice for the creation of patent, three-dimensional endothelial cell-based microcirculatory networks," *Biomicrofluidics* **5**, 034115 (2011).
- ¹⁰J. G. Truslow and J. Tien, "Perfusion systems that minimize vascular volume fraction in engineered tissues," *Biomicrofluidics* **5**, 22201 (2011).
- ¹¹N. L. Jeon, "In vitro formation and characterization of a perfusable three-dimensional tubular capillary network in microfluidic devices," *Lab Chip* **12**, 2815–2822 (2012).

- ¹²S. G. Darby, M. R. Moore, T. A. Friedlander, D. K. Schaffer, R. S. Reiserer *et al.*, "A metering rotary nanopump for microfluidic systems," *Lab Chip* **10**, 3218–3226 (2010).
- ¹³B. Zhang, J. V. Green, S. K. Murthy, and M. Radisic, "Label-free enrichment of functional cardiomyocytes using microfluidic deterministic lateral flow displacement," *PLoS ONE* **7**, e37619 (2012).
- ¹⁴D. T. Eddington, "Chips & Tips: In-line microfluidic bubble trap," *Lab Chip* (published online), available at http://www.rsc.org/Publishing/Journals/lc/bubble_trap.asp.
- ¹⁵L. K. Fiddes, N. Raz, S. Srigunapalan, E. Tumarkan, C. A. Simmons *et al.*, "A circular cross-section PDMS microfluidics system for replication of cardiovascular flow conditions," *Biomaterials* **31**, 3459–3464 (2010).
- ¹⁶J. Huynh, N. Nishimura, K. Rana, J. M. Peloquin, J. P. Califano *et al.*, "Age-related intimal stiffening enhances endothelial permeability and leukocyte transmigration," *Sci. Trans. Med.* **3**, 112ra122 (2011).
- ¹⁷W. C. Aird, "Phenotypic heterogeneity of the endothelium: I. Structure, function, and mechanisms," *Circ. Res.* **100**, 158–173 (2007).
- ¹⁸D. L. Kellogg, J. L. Zhao, U. Coey, and J. V. Green, "Acetylcholine-induced vasodilation is mediated by nitric oxide and prostaglandins in human skin," *J. Appl. Physiol.* **98**, 629–632 (2005).
- ¹⁹T. Chataigneau, M. Félétou, P. L. Huang, M. C. Fishman, J. Duhault *et al.*, "Acetylcholine-induced relaxation in blood vessels from endothelial nitric oxide synthase knockout mice," *Br. J. Pharmacol.* **126**, 219–226 (1999).
- ²⁰A. Gunther, S. Yasotharan, A. Vagaon, C. Lochovsky, S. Pinto *et al.*, "A microfluidic platform for probing small artery structure and function," *Lab Chip* **10**, 2341–2349 (2010).
- ²¹S. Atar, Y. Ye, Y. Lin, S. Y. Freeberg, S. P. Nishi *et al.*, "Atorvastatin-induced cardioprotection is mediated by increasing inducible nitric oxide synthase and consequent S-nitrosylation of cyclooxygenase-2," *Am. J. Physiol. Heart Circ. Physiol.* **290**, H1960–H1968 (2006).
- ²²M. F. Mahmoud, M. El-Nagar, and H. M. El-Bassossy, "Anti-inflammatory effect of atorvastatin on vascular reactivity and insulin resistance in fructose fed rats," *Arch. Pharmacol. Res.* **35**, 155–162 (2012).
- ²³V. Dishy, G. Sofowora, P. A. Harris, M. Kandcer, F. Zhan *et al.*, "The effect of sildenafil on nitric oxide-mediated vasodilation in healthy men," *Clin. Pharmacol. Ther.* **70**, 270–279 (2001).
- ²⁴C. Mammi, D. Pastore, M. F. Lombardo, F. Ferrelli, M. Caprio *et al.*, "Sildenafil reduces insulin-resistance in human endothelial cells," *PLoS ONE* **6**, e14542 (2011).
- ²⁵J. D. Buxbaum, M. Oishi, H. I. Chen, R. Pinkas-Kramarski, E. A. Jaffe *et al.*, "Cholinergic agonists and interleukin 1 regulate processing and secretion of the Alzheimer beta/A4 amyloid protein precursor," *Proc. Natl. Acad. Sci. U.S.A.* **89**, 10075–10078 (1992).
- ²⁶G. Jackson, N. Benjamin, N. Jackson, and M. J. Allen, "Effects of sildenafil citrate on human hemodynamics," *Am. J. Cardiol.* **83**, 13–20 (1999).
- ²⁷A. Das, L. Xi, and R. C. Kukreja, "Phosphodiesterase-5 inhibitor sildenafil preconditions adult cardiac myocytes against necrosis and apoptosis. Essential role of nitric oxide signaling," *J. Biol. Chem.* **280**, 12944–12955 (2005).
- ²⁸J. B. Salom, M. C. Burguete, F. J. Pérez-Asensio, M. Castelló-Ruiz, G. Torregrosa *et al.*, "Relaxant effect of sildenafil in the rabbit basilar artery," *Vasc. Pharmacol.* **44**, 10–16 (2006).
- ²⁹S. H. Francis, J. L. Busch, J. D. Corbin, and D. Sibley, "cGMP-dependent protein kinases and cGMP phosphodiesterases in nitric oxide and cGMP action," *Pharmacol. Rev.* **62**, 525–563 (2010).
- ³⁰K.-W. Lee, D. B. Stolz, and Y. Wang, "Substantial expression of mature elastin in arterial constructs," *Proc. Natl. Acad. Sci. U.S.A.* **108**, 2705–2710 (2011).
- ³¹L.-M. Li, X.-Y. Wang, L.-S. Hu, R.-S. Chen, Y. Huang *et al.*, "Vascular lumen simulation and highly-sensitive nitric oxide detection using three-dimensional gelatin chip coupled to TiC/C nanowire arrays microelectrode," *Lab Chip* **12**, 4249–4256 (2012).